

# Transverse-Mode Structure of a Phase-Conjugate Oscillator Based on Brillouin-Enhanced Four-Wave Mixing

MARK D. SKELDON AND ROBERT W. BOYD

**Abstract**—A phase-conjugate oscillator consisting of a phase-conjugate mirror and a conventional mirror has been constructed. The phase-conjugate mirror is based on a Brillouin-enhanced four-wave mixing process and produces a conjugate wave with no frequency shift and with a reflectivity greater than 100 percent. The beam divergence and near field spot size of this oscillator have been measured for various cavity lengths and conventional mirror radii of curvature. A theoretical analysis of the mode structure of this oscillator has been performed assuming a Gaussian reflectivity profile for the phase-conjugate mirror. The measurements are in good agreement with the predictions of this model.

## INTRODUCTION

ONE of the applications of optical phase conjugation is in the construction of phase-conjugate resonators consisting of a phase-conjugate mirror (PCM) and a conventional mirror. A laser that incorporates a phase-conjugate resonator can produce an output beam whose quality is unaffected by distortions introduced by the internal elements of the laser. The mode structure of a phase-conjugate resonator has been analyzed theoretically in several previous studies [1]–[20]; however, detailed experimental studies of the mode structure have been very limited. In this paper, we present the results of our experimental investigation of the output beam characteristics of a phase-conjugate oscillator for various cavity lengths and radii of curvature of the conventional mirror. The PCM used in our phase-conjugate oscillator is one based on Brillouin-enhanced four-wave mixing and has been discussed previously [21], [22]. We find good agreement between our measurements of the output beam characteristics and the predictions of a theoretical model of the mode characteristics of a phase-conjugate oscillator. We have studied both cases in which the higher order modes experience high loss and hence oscillation is primarily in the lowest order mode, and cases in which the presence of higher order modes is important.

## THEORY

We model the phase-conjugate resonator as consisting of a PCM with a Gaussian reflectivity profile in the trans-

verse direction and a conventional mirror separated from the PCM by a distance that we refer to as the cavity length. Our treatment is similar to that presented previously by Pepper [4] and by Siegman *et al.* [15]. The Gaussian reflectivity profile is important in determining the mode structure of this type of resonator. In fact, in practice, PCM's often have Gaussian reflectivity profiles because they are pumped by laser beams that have Gaussian intensity profiles. In addition, we assume that the PCM produces no frequency shift on reflection and has a total reflectivity greater than 100 percent, thus acting as a gain element in the resonator. These assumptions are well satisfied in our experimental oscillator.

To determine the allowed mode structure of this phase-conjugate resonator, we use the *ABCD* ray matrix technique [23]. We begin by developing the *ABCD* ray-transfer matrix that corresponds to reflection from a PCM with a Gaussian reflectivity profile. We assume that the field incident on the PCM has the form

$$E_i(r, z, t) = e_i(r) \exp \left[ i \left( \omega t - kz - \frac{kr^2}{2q_i} \right) \right] \quad (1)$$

where the complex beam parameter  $q_i$  of the incident beam is given by

$$\frac{1}{q_i} = \frac{1}{\rho_i} - \frac{i\lambda}{\pi w_i^2} \quad (2)$$

and  $\rho_i$  is the radius of curvature and  $w_i$  is the spot size of the incident field with wavelength  $\lambda$ . For a given mode, knowledge of the complex beam parameter  $q$  at any plane, in conjunction with the beam propagation laws, uniquely determines the beam characteristics for that mode everywhere in free space. As mentioned above, we assume that the amplitude reflectivity  $\mu$  of the PCM varies in the transverse direction according to

$$\mu(r) = \mu_0 \exp \left[ -\frac{r^2}{a^2} \right] \quad (3)$$

where  $a$  is the characteristic width of the reflectivity profile and  $\mu_0$  is the reflectivity on axis. We assume that the on-axis reflectivity  $\mu_0$  is a constant independent of the incident field intensity (i.e., we ignore saturation effects). The field reflected from the PCM will then be given by

Manuscript received February 1, 1988; revised May 3, 1988. This work was supported by the sponsors of the New York State Center for Advanced Optical Technology.

The authors are with the Institute of Optics, University of Rochester, Rochester, NY 14627.

IEEE Log Number 8825899.

the complex conjugate of the incident field's complex amplitude (1), multiplied by the reflectivity profile of the PCM (3), that is, by

$$E_r(r, z, t) = \mu_0 \epsilon_i^*(r) \exp \left[ i \left( \omega t + kz - \frac{kr^2}{2q_r} \right) \right]. \quad (4)$$

Here the complex beam parameter  $q_r$  of the reflected wave is given by

$$\frac{1}{q_r} = -\frac{1}{\rho_i} - \frac{i\lambda}{\pi} \left[ \frac{1}{w_i^2} + \frac{1}{a^2} \right], \quad (5)$$

that is, by

$$\frac{1}{q_r} = -\frac{1}{q_i^*} - \frac{i\lambda}{\pi a^2}. \quad (6)$$

This last expression relates the complex beam parameters of the incident and reflected fields, and hence completely describes reflection of a Gaussian beam from a PCM. Note that the action of the PCM is twofold: the sign of the radius of curvature  $\rho$  is reversed and, because of the Gaussian reflectivity profile, the spot size of the beam is modified on reflection. The change in sign of  $\rho$  upon reflection is a consequence of the sign convention we have used in (1), (2), and (4); in fact, the actual phase front remains unchanged upon reflection from a PCM. The spot size, on the other hand, changes discontinuously upon reflection from the PCM, implying that the cavity mode consists of two different Gaussian beams, one traveling to the right and one traveling to the left. For large values of  $a$  ( $a \gg w_i$ ), the  $1/a^2$  term in (5) can be neglected and the left- and right-going beams acquire identical phase fronts and beam diameters everywhere.

For an optical system that can be described by a paraxial  $ABCD$  ray-transfer matrix and that contains one PCM, propagation of a Gaussian beam through the system results in the following relationship between the incident complex beam parameter  $q_i$  and the reflected beam parameter  $q_r$  [24]:

$$\frac{1}{q_r} = \frac{C + \frac{D}{q_i^*}}{A + \frac{B}{q_i^*}}. \quad (7)$$

Here, complex conjugation of the complex beam parameter on the right-hand side of this equation is required since the system includes one reflection from a PCM. From (6) and (7), we see that the  $ABCD$  matrix that corresponds to reflection from a PCM with a Gaussian reflectivity profile is given by

$$\begin{bmatrix} A & B \\ C & D \end{bmatrix} = \begin{bmatrix} 1 & 0 \\ -\frac{i\lambda}{\pi a^2} & -1 \end{bmatrix}. \quad (8)$$

With this matrix, we are now able to calculate the complex beam parameter  $q$  that reproduces itself after one

roundtrip through a phase-conjugate resonator. For example, let us consider the case of a phase-conjugate resonator consisting of a PCM with a Gaussian reflectivity profile and a conventional mirror with radius of curvature  $R$  located a distance  $L$  from the PCM. If we begin the analysis at the PCM, then the total  $ABCD$  matrix for this system is given by the matrix product

$$\begin{bmatrix} A & B \\ C & D \end{bmatrix} = \begin{bmatrix} 1 & L \\ 0 & 1 \end{bmatrix} \begin{bmatrix} 1 & 0 \\ -\frac{2}{R} & 1 \end{bmatrix} \begin{bmatrix} 1 & L \\ 0 & 1 \end{bmatrix} \begin{bmatrix} 1 & 0 \\ -\frac{i\lambda}{\pi a^2} & -1 \end{bmatrix}. \quad (9)$$

The four matrices on the right-hand side correspond from right to left to reflection from the PCM, propagation to the conventional mirror, reflection from the conventional mirror, and propagation back to the PCM. The requirement that the resonator be geometrically stable implies that the  $q$  parameter must come back to itself (i.e.,  $q_i = q_r$ ) after one roundtrip. We must therefore find the solution of (7) with  $q_i = q_r$  with the quantities  $A$ ,  $B$ ,  $C$ , and  $D$  given by (9). The real and imaginary parts of (7) constitute two equations in two unknowns: the radius of curvature  $\rho$  and the spot size  $w$  of the beam incident on the PCM. We note that if the PCM had an infinite extent in the transverse direction (i.e., if  $a \rightarrow \infty$ ), then the imaginary part of (7) would give no information and there would be an infinite number of allowed modes for this resonator, each having radius of curvature  $R$  but an arbitrary spot size at the conventional mirror. The solution for the spot size  $w_{i,\text{pcm}}$  and radius of curvature  $\rho_{i,\text{pcm}}$  of the beam incident on the PCM that reproduces itself after one roundtrip is given by

$$w_{i,\text{pcm}}^2 = \frac{g^2}{2a^2} + g \left[ \frac{g^2}{4a^4} + 1 \right]^{1/2} \quad (10a)$$

and

$$\rho_{i,\text{pcm}} = \frac{2L \left( 1 - \frac{L}{R} \right)}{1 - \frac{2L}{R}}. \quad (10b)$$

where  $g = |2L\lambda/\pi (1 - L/R)|$ . After reflection from the PCM, the new spot size  $w_{r,\text{pcm}}$  and radius of curvature  $\rho_{r,\text{pcm}}$  at the PCM will be given according to (5) by

$$\frac{1}{w_{r,\text{pcm}}^2} = \frac{1}{w_{i,\text{pcm}}^2} + \frac{1}{a^2} \quad (11a)$$

and

$$\rho_{r,\text{pcm}} = -\rho_{i,\text{pcm}}. \quad (11b)$$

Note that these solutions depend on only four variables: the cavity length  $L$ , the radius of curvature  $R$  of the output coupler, the wavelength  $\lambda$  of the light used, and the width of the Gaussian reflectivity profile  $a$ . These variables are determined by the experimental conditions. Note also that

valid solutions are obtained with no restriction on the cavity length  $L$  or the sign of the radius of curvature  $R$  of the output coupler, unlike for the case of conventional resonators.

With these solutions [(10) and (11)] and the standard beam propagation laws, we can determine the beam parameters of the allowed mode everywhere in space. In particular, we obtain for the spot size  $w_{i,cm}$  and radius of curvature  $\rho_{i,cm}$  of the beam incident on the conventional mirror

$$w_{i,cm}^2 = \frac{L\lambda}{\pi|1 - L/R|} \left[ 1 + \frac{q^2}{4a^4} \right]^{1/2} \quad (12a)$$

and

$$\rho_{i,cm} = \left[ \frac{1}{R} + \frac{\lambda}{\pi a^2} \left( 1 - \frac{L}{R} \right)^2 \left[ 1 + \frac{q^2}{4a^4} \right]^{-1/2} \right]^{-1} \quad (12b)$$

After reflection from the conventional mirror, the new spot size  $w_{r,cm}$  and radius of curvature  $\rho_{r,cm}$  of the beam at the conventional mirror will be given by

$$w_{r,cm} = w_{i,cm} \quad (13a)$$

and

$$\rho_{r,cm} = - \left[ \frac{1}{R} - \frac{\lambda}{\pi a^2} \left( 1 - \frac{L}{R} \right)^2 \left[ 1 + \frac{q^2}{4a^4} \right]^{-1/2} \right]^{-1} \quad (13b)$$

Note that at the conventional mirror, the spot size is continuous on reflection and the radius of curvature of the mode is discontinuous on reflection. In general, the wavefront curvature of the mode at the conventional mirror does not match the curvature  $R$  of the conventional mirror; however, the wavefront curvature does approach the curvature of the conventional mirror in the limit of large values of  $a$  or when the cavity length  $L$  approaches  $R$ . Note, also, that these solutions [(12) and (13)] are slightly different from the solutions obtained for a phase-conjugate resonator modeled with a conventional mirror and an "ideal" PCM with a Gaussian filter placed in front of it [6], [12], [14], [18].

In Fig. 1, we show phase-conjugate resonators with conventional mirrors having different curvatures. In Fig. 1 (a), (b) and (c), we show the mode for the case of a very large phase-conjugate mirror ( $a \rightarrow \infty$ ) with a flat, convex, and concave conventional mirror, respectively. In Fig. 1(d), we show the mode structure of a phase-conjugate resonator having a flat conventional mirror and with a finite width  $a$  of the Gaussian reflectivity profile. In this case, the mode consists of left- and right-going beams having different beam parameters, as shown by the solid lines. The dashed lines in Fig. 1(d) depict the virtual beam waist of the left-going beam in the resonator.

In Figs. 2, 3, and 4, we show graphically the location of the beam waist measured with respect to the location of the PCM, and the spot size of the beam waist as a

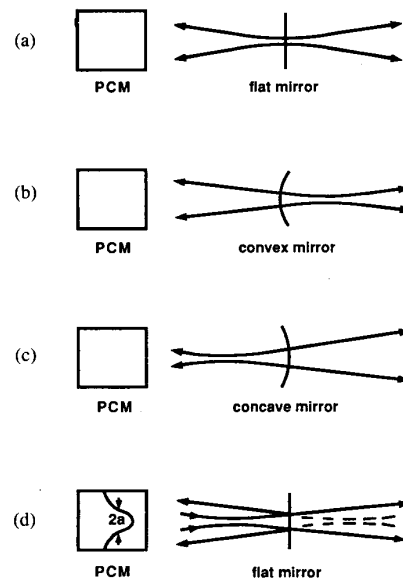


Fig. 1. Phase-conjugate resonators consisting of a phase-conjugate mirror (PCM) and an (a) flat, (b) convex, and (c) concave conventional mirror. In (d), the PCM has a Gaussian reflectivity profile of width  $2a$ . Consequently, the oscillating mode of this resonator consists of left- and right-going beams having different beam parameters, shown by the solid lines. The dashed lines depict the virtual beam waist of the left-going beam.

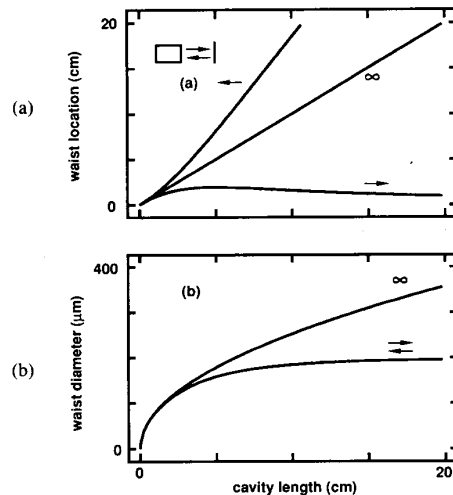


Fig. 2. (a) Beam waist location measured with respect to the location of the phase-conjugate mirror and (b) beam waist diameter plotted versus cavity length for a phase-conjugate resonator consisting of a flat conventional mirror and a PCM with Gaussian reflectivity profiles  $a = \infty$  and  $a = 0.01$  cm for a wavelength of  $0.5 \mu\text{m}$ . For  $a = \infty$ , the left- and right-going beams are identical, and the plots are labeled by  $\infty$ . For  $a = 0.01$  cm, the plot for the right-going beam is indicated by the right arrow, and the plot for the left-going beam is indicated by the left arrow.

function of cavity length for three different phase-conjugate resonators for  $\lambda = 0.5 \mu\text{m}$  and with conventional mirror radii of curvature equal to  $\infty$ ,  $-10$  cm and  $+10$  cm, respectively. In each case, we show the waist location and size for the two Gaussian beams in the resonator, the right-going beam (right arrow) and left-going beam

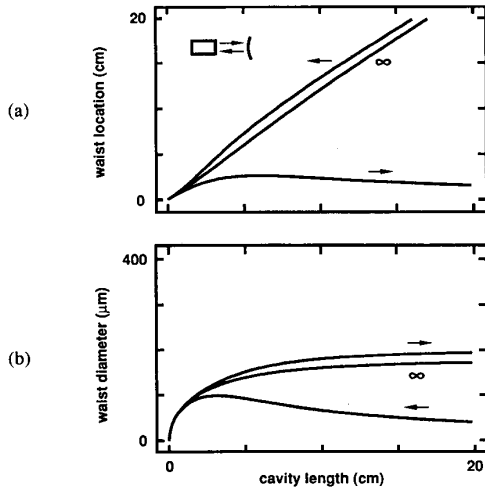


Fig. 3. Same as Fig. 2, but for a conventional mirror with a  $-10$  cm radius of curvature.

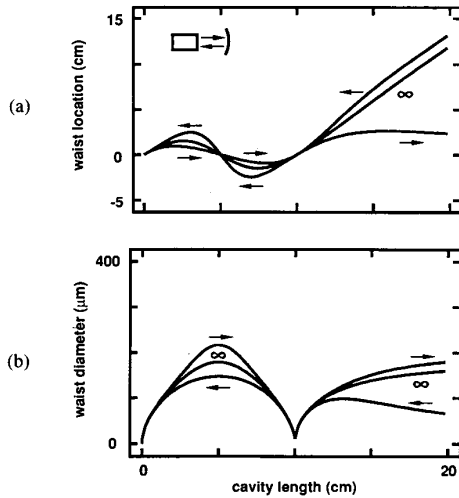


Fig. 4. Same as Fig. 2, but for a conventional mirror with a  $+10$  cm radius of curvature.

(left arrow), for values of the Gaussian reflectivity profile of width  $a = \infty$  and  $a = 0.01$  cm. For the case  $a = \infty$ , the right- and left-going beams are identical.

In general, there are other possible modes such as off-axis modes that reproduce in two roundtrips; however, these modes are neglected here since they have a higher loss due to the assumed reflectivity profile, and hence, are not expected to be present in our experimental oscillator.

The above derivation of the allowed modes of a phase-conjugate resonator assumed oscillation of the lowest order Gaussian mode. To examine the effects of the higher order Hermite-Gaussian modes, we calculate the roundtrip diffraction losses for these modes. These Hermite-Gaussian modes have the form

$$E_{nm} = a_{nm} V^{n+m} H_n \left( \frac{2x}{V} \right) H_m \left( \frac{2y}{V} \right) \exp \left[ -\frac{ik(x^2 + y^2)}{2q} \right] \quad (14)$$

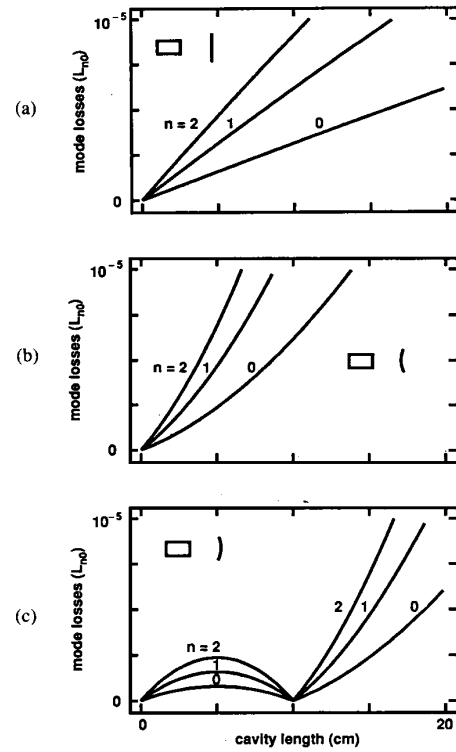


Fig. 5. Mode loss per roundtrip plotted versus cavity length for the three Hermite-Gaussian modes with  $nm = 00, 10,$  and  $20$  for a phase-conjugate resonator with a conventional mirror radius of curvature equal to (a) infinity, (b)  $-10$  cm, and (c)  $+10$  cm, and a PCM with Gaussian reflectivity profile  $a = 0.1$  cm for a wavelength of  $0.5 \mu\text{m}$ .

where  $V$  is the complex spot size [24] and  $a_{nm}$  is the amplitude of mode  $nm$ . The amplitude of this mode will decrease after one roundtrip through the cavity by the ratio [5], [15]

$$\left| \frac{a_{nm,f}}{a_{nm,i}} \right| = \left\{ \left[ 1 + \left( \frac{g}{a^2} \right)^2 \right]^{1/2} + \frac{g}{a^2} \right\}^{-(n+m)-1} \quad (15)$$

where  $a_{nm,i}$  is the initial mode amplitude and  $a_{nm,f}$  is the final mode amplitude after the roundtrip through the cavity. The geometrical loss per roundtrip is then given by  $L_{nm} = 1 - a_{nm,f}/a_{nm,i}$  and depends on the loss for the lowest order mode. For the three resonators studied, the geometrical losses for modes  $nm = 00, 10,$  and  $20$  are shown graphically in Fig. 5 for a wavelength  $\lambda = 0.5 \mu\text{m}$  and for a Gaussian reflectivity profile of width  $a = 0.1$  cm. We see from (15) that for the case of large  $a$  or when the cavity length equals the conventional mirror radius of curvature ( $g = 0$ ), the losses for all modes are equal. For these cases, the resonator cannot discriminate against higher order modes, and higher order modes may be important in the analysis. In addition to the above considerations, in the experiment to be discussed, mode discrimination is enhanced by the fact that the PCM is only reflecting for approximately 10 ns, allowing only the lowest loss modes time to build up from noise.

## EXPERIMENT

Experimental studies of the mode properties of a phase-conjugate oscillator were performed on an oscillator incorporating a PCM based on Brillouin-enhanced four-wave mixing [21], [22]. The experimental setup for this phase-conjugate oscillator is shown in Fig. 6. The forward pump at frequency  $\omega$  for the four-wave mixing process is generated by a  $Q$ -switched frequency-doubled Nd:YAG laser producing about 25 mJ of energy in a 10 ns pulse width, with a 2 mm diameter spot size (measured to the  $1/e^2$  intensity point) at the front window of the  $\text{CS}_2$  four-wave mixing cell. The backward pump wave is generated by a stimulated Brillouin scattering PCM filled with the liquid glycerol and has a frequency ( $\omega - 2\Omega$ ) shifted downward by twice the Brillouin frequency shift ( $\Omega$ ) of the four-wave mixing medium ( $\text{CS}_2$ ). With this choice of frequencies for the four-wave mixing process, gain is produced at the frequency  $\omega - \Omega$  due to a four-wave mixing process that is mediated by intense acoustic waves. The forward pump wave for the four-wave mixing process has an intensity near the stimulated Brillouin scattering threshold for  $\text{CS}_2$ . The weak stimulated Brillouin scattering generated by this forward pump wave provides the seed photons at the Stokes-shifted frequency  $\omega - \Omega$  to initiate oscillation between the PCM and the conventional mirror. The pump waves used for the four-wave mixing PCM were  $\text{TEM}_{00}$  Gaussian, which produced a PCM with a Gaussian reflectivity profile in the transverse direction with  $a = 0.1$  cm. The PCM has a reflectivity greater than 100 percent and provides gain for the oscillator. Conventional mirrors with radii of curvature  $R = \infty$ ,  $-10$  cm, and  $+10$  cm were used as output couplers for this phase-conjugate resonator, and cavity lengths were varied from approximately 5 to 20 cm. Short cavity lengths were limited by the finite size of the PCM (the four-wave mixing cell had a length of 3 cm) and the optics required to form the oscillator. Long cavity lengths were limited by the number of roundtrips available for the oscillation to build up from noise. The duration of the PCM reflectivity was approximately equal to the pump laser pulse width (10 ns FWHM). Typically, fewer than ten roundtrips were available for the oscillator to initiate from noise, sample the cavity, and form a cavity mode. The phase-conjugate oscillator was operated slightly above threshold and was not optimized for efficiency; thus, the output energy from the oscillator was low (less than  $10 \mu\text{J}$  per pulse). The pulse width of the phase-conjugate oscillator was approximately 5 ns and had a smooth temporal profile similar to the temporal profile of the pump laser. The spot sizes of the output beams from these oscillators were measured both in the near field and in the far field for several values of the cavity length. Fig. 7 shows the output beam divergences from the phase-conjugate oscillators studied. Fig. 8 shows the near field spot sizes measured at a plane inside the phase-conjugate oscillator. Typical error bars associated with the spot size measurements are shown in each plot. These measurements are compared to the the-

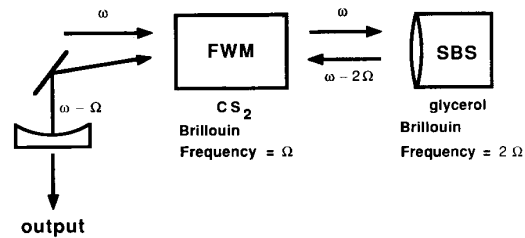


Fig. 6. Experimental setup for a phase-conjugate oscillator consisting of a conventional mirror and an amplifying phase-conjugate mirror based on Brillouin-enhanced four-wave mixing.

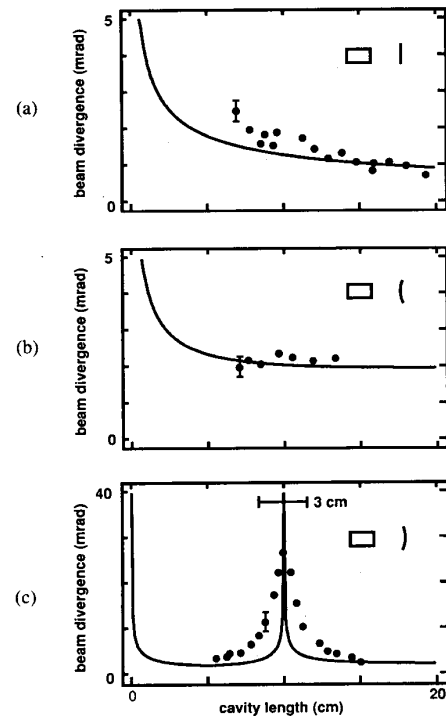


Fig. 7. Measured beam divergence plotted versus cavity length for a phase-conjugate oscillator with a conventional mirror radius of curvature equal to (a) infinity, (b)  $-10$  cm, and (c)  $+10$  cm. The solid curve shows the predictions of the theory presented in the text for  $a = 0.1$  cm.

oretical analysis above (solid line in the figures) assuming oscillation of the lowest order Gaussian mode and  $a \gg w_{i,\text{pcm}}$ .

For the case of a phase-conjugate oscillator with a flat conventional mirror, we see close agreement between the lowest order Gaussian mode theory and the experimental measurements for long cavity lengths [Figs. 7(a) and (8a)]. For shorter cavity lengths, however, the divergence is greater than the prediction of the lowest order mode theory, suggesting that multitransverse-mode oscillation is occurring. For shorter cavity lengths, the losses for higher order modes are lower (see Fig. 5), and in addition, there are more roundtrips through the oscillator during which higher order modes can grow. Hence, the beam divergence for short cavity lengths may have contributions from the presence of higher order modes.

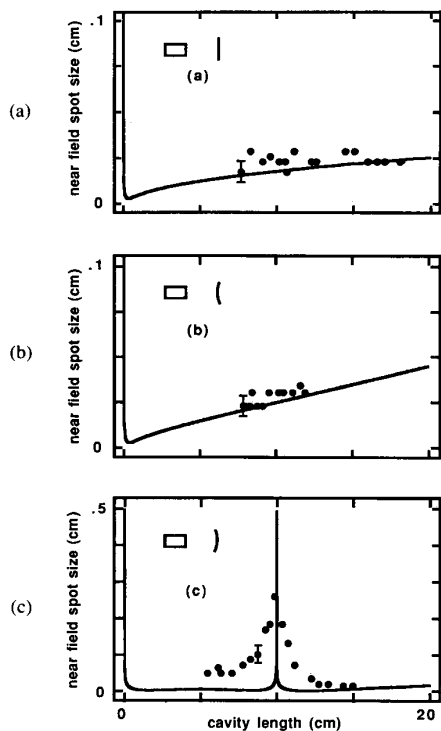


Fig. 8. Near field spot size measured at a fixed plane inside the phase-conjugate oscillator plotted versus cavity length for a conventional mirror radius of curvature equal to (a) infinity, (b)  $-10$  cm, and (c)  $+10$  cm. The solid curve shows the predictions of the theory presented in the text for  $a = 0.1$  cm.

For the case of a phase-conjugate oscillator with a  $-10$  cm radius of curvature, we see better agreement between the output beam measurements and the low-order mode theory for all cavity lengths [Figs. 7(b) and 8(b)]. For short cavity lengths, in this case, the additional losses for the higher order modes (see Fig. 5) may be sufficient to prevent these modes from building up.

Finally, for the case of a phase-conjugate oscillator with a  $+10$  cm radius-of-curvature conventional mirror, we see that for all cavity lengths, the output beam divergence is greater than that of a lowest order Gaussian mode. Also, when the cavity length equals the radius of curvature of the conventional mirror, the beam waist is located inside the PCM (see Fig. 4), the beam waist diameter becomes very small, and the losses for all modes are equal [see Fig. 5(c)]. Hence, for the case when the cavity length is approximately equal to the radius of curvature of the conventional mirror, there is little or no mode discrimination, and we expect nondiffraction-limited output from the oscillator. We see from Figs. 7(c) and 8(c) that the output beam divergence exceeds the fundamental-mode beam divergence by a factor of approximately three, suggesting that approximately ten modes are oscillating.

For all of our oscillators, we have measured the cavity length from the center of the 3 cm four-wave mixing cell used as the PCM. This definition of the cavity length is consistent with that used by other authors [12], [15] and

gives the best fit to the data, as can be seen for the case of the cavity length equal to the radius of curvature of the conventional mirror [Fig. 7(c)].

In conclusion, we have operated several phase-conjugate oscillators consisting of a conventional mirror and a PCM with gain based on Brillouin-enhanced four-wave mixing. We have measured the output beam parameters of these oscillators both in the near and far fields for various cavity lengths. We have calculated the allowed mode structure of these oscillators by assuming that the PCM had a Gaussian reflectivity profile in the transverse dimension, and have compared our measurements to a theoretical analysis that assumes oscillation of a low-order Gaussian mode. Good agreement between the theory and experiment is obtained when we consider the role of the higher order Hermite-Gaussian modes in these oscillators.

#### ACKNOWLEDGMENT

Discussions of the Brillouin-enhanced four-wave mixing process with P. Narum are gratefully acknowledged.

#### REFERENCES

- [1] I. M. Bel'dyugin, M. G. Galushkin, and E. M. Zemskov, "Properties of resonators with wavefront-reversing mirrors," *Sov. J. Quantum Electron.*, vol. 9, pp. 20-23, 1979.
- [2] J. Auyeung, D. Fekete, D. M. Pepper, and A. Yariv, "A theoretical and experimental investigation of the modes of optical resonators with phase-conjugate mirrors," *IEEE J. Quantum Electron.*, vol. QE-15, pp. 1180-1187, 1979.
- [3] I. M. Bel'dyugin and E. M. Zemskov, "Theory of resonators with wavefront-reversing mirrors," *Sov. J. Quantum Electron.*, vol. 9, pp. 1198-1199, 1979.
- [4] D. M. Pepper, Ph.D. dissertation, California Inst. Technol., Pasadena, Michigan Univ. Microfilm 8014305, 1980, Appendix 7B "PCM ray matrix assuming spatially-dependent Gaussian pump beams," pp. 310-318. See also R. Trebino and A. E. Siegman, "Phase-conjugate reflection at arbitrary angles using TEM $_{\infty}$  pump beams," *Opt. Commun.*, vol. 32, pp. 1-4, 1980.
- [5] P. A. Belanger, A. Hardy, and A. E. Siegman, "Resonant modes of optical cavities with phase conjugate mirrors: Higher order modes," *Appl. Opt.*, vol. 19, pp. 479-480, 1980.
- [6] —, "Resonant modes of optical cavities with phase-conjugate mirrors," *Appl. Opt.*, vol. 19, pp. 602-609, 1980.
- [7] J. F. Lam and W. P. Brown, "Optical resonators with phase-conjugate mirrors," *Opt. Lett.*, vol. 5, pp. 61-63, 1980.
- [8] M. G. Reznikov and A. I. Khizhnyak, "Properties of a resonator with a wavefront-reversing mirror," *Sov. J. Quantum Electron.*, vol. 10, pp. 633-634, 1980.
- [9] I. M. Bel'dyugin and E. M. Zemskov, "Calculation of the field in a laser resonator with a wavefront-reversing mirror," *Sov. J. Quantum Electron.*, vol. 10, pp. 764-765, 1980.
- [10] A. Hardy and S. Hochhauser, "Phase-conjugate resonators with intracavity amplitude perturbations," *Appl. Opt.*, vol. 21, pp. 1118-1121, 1982.
- [11] A. Hardy, P. A. Belanger, and A. E. Siegman, "Orthogonality properties of phase conjugate optical resonators," *Appl. Opt.*, vol. 21, pp. 1122-1124, 1982.
- [12] P. A. Belanger, "Phase conjugation and optical resonators," *Opt. Eng.*, vol. 21, pp. 266-270, 1982.
- [13] A. Hardy and S. Hochhauser, "Higher-order modes of phase conjugate resonators," *Appl. Opt.*, vol. 21, pp. 2330-2338, 1982.
- [14] G. Giuliani, M. M. Denariez-Roberge, and P. A. Belanger, "Transverse modes of a stimulated scattering phase-conjugate resonator," *Appl. Opt.*, vol. 21, pp. 3719-3724, 1982.
- [15] A. E. Siegman, P. A. Belanger, and A. Hardy, in *Optical Phase Conjugation*, R. A. Fisher, Ed. New York: Academic, 1982, ch. 10.
- [16] P. A. Belanger, C. Pare, and M. Piche, "Modes of phase-conjugate

- resonators with bounded mirrors," *J. Opt. Soc. Amer.*, vol. 73, pp. 567-571, 1983.
- [17] P. Yeh, "Theory of phase-conjugate oscillators," *J. Opt. Soc. Amer. A*, vol. 2, pp. 727-730, 1985.
- [18] B. Ya. Zel'dovich, N. F. Pilipetsky, and V. V. Shunov, in *Principles of Phase Conjugation*. New York: Springer-Verlag, 1985, ch. 8.
- [19] G. Reiner, P. Meystre, and E. M. Wright, "Transverse dynamics of a phase-conjugate resonator. I: Sluggish nonlinear medium," *J. Opt. Soc. Amer. B*, vol. 4, pp. 675-686, 1987.
- [20] E. S. Kim, C. H. Cho, I. E. Young, and H. K. Park, "Orthogonality properties of transverse eigenmodes of phase conjugate optical resonators," *IEEE J. Quantum Electron.*, vol. QE-23, pp. 2047-2050, 1987.
- [21] M. D. Skeldon, P. Narum, and R. W. Boyd, "Phase conjugate mirror with gain based on Brillouin scattering," *Proc. SPIE*, vol. 739, pp. 57-63, 1987.
- [22] —, "Non-frequency-shifted, high-fidelity phase conjugation with aberrated pump waves by Brillouin-enhanced four-wave mixing," *Opt. Lett.*, vol. 12, pp. 343-345, 1987.
- [23] H. Kogelnik and T. Li, "Laser beams and resonators," *Appl. Opt.*, vol. 5, pp. 1550-1566, 1966.
- [24] A. E. Siegman, in *Lasers*. New York: McGraw-Hill, 1987, ch. 20.

**Mark D. Skeldon**, photograph and biography not available at the time of publication.

**Robert W. Boyd**, photograph and biography not available at the time of publication.

---